

# Inferring intermediate states by leveraging the many-body Arrhenius law

Vishwajeet Kumar,<sup>1,2</sup> Arnab Pal,<sup>1,2,\*</sup> and Ohad Shpielberg<sup>3,4,†</sup>

<sup>1</sup>*The Institute of Mathematical Sciences, CIT Campus, Taramani, Chennai 600113, India*

<sup>2</sup>*Homi Bhabha National Institute, Training School Complex, Anushakti Nagar, Mumbai 400094, India*

<sup>3</sup>*Department of Mathematics and Physics, University of Haifa at Oranim, Kiryat Tivon 3600600, Israel*

<sup>4</sup>*Haifa Research Center for Theoretical Physics and Astrophysics,  
University of Haifa, Abba Khoushy Ave 199, Haifa 3498838, Israel*

Metastable states appear as long-lived intermediate states in various natural transport phenomena which are governed by energy landscapes. Moreover, they dominate a system's evolution in deciding the selective outcome or shedding light on the preferred mechanism on how a system explores the energy landscape. It is thus crucial to develop techniques to quantify these metastabilities hence uncovering key details of the energy landscape. Here, we propose a powerful method by leveraging a many-body Arrhenius law that detects the metastabilities in an escape problem, involving interacting particles with excluded volume confined to a complex energy landscape. Observing transport in colloidal systems or translocation of macromolecules through biological pores can be an ideal test bed to verify our results.

PACS numbers: Valid PACS appear here

## INTRODUCTION

The Arrhenius law (AL) is a cornerstone of physical chemistry. It captures the temperature dependence on the rate of chemical reactions, and helps to quantitatively explain why milk turns sour quicker outside the fridge. It was the seminal work of Kramers, providing the underlying formalism that revealed the ubiquity of the AL throughout science and engineering [1]. More than a century following Arrhenius' experimental observation, the physics of activation still remains a vibrant topic of research [2–17]. In its simplest form, the Kramers problem consists of an overdamped particle in a trapping potential, coupled to thermal bath at temperature  $T$ . To escape the trapping potential, the particle needs to overcome the energy barrier denoted by  $\Delta U$  - the activation energy. In the limit of deep traps  $\beta\Delta U \gg 1$ , the single particle escape rate is captured by the AL

$$\Phi_{\text{SP}} = \frac{1}{\tau_0} e^{-\beta\Delta U}, \quad (1)$$

where  $k_B$  is the Boltzmann constant,  $\beta = 1/k_B T$ , and the sub-exponential contribution  $\tau_0$  is a microscopic time scale that depends on the details of the trap.

Of prime importance is the inverse problem: extracting the features of the energy landscape or more precisely, the details of the potential trap from the escape time statistics. One aspect of the inverse problem, prevalent in the theory of chemical dynamics, is predicting the value of the energy barrier  $\Delta U$  by interpreting experimental data. Such an activation process may extend beyond the standard Kramers setup, and involve a conformational or configurational transition as motion along the reaction

coordinate in a rugged energy landscape. See [18] for details. A second aspect of the inverse problem is inferring the coordinates and number of local minima in the energy landscape. The local minima can be identified as long-lived states, or metastabilities, where the system spends significant time. Identifying these metastabilities enables the reduction of the system's state space by filtering out fast degrees of freedom, a crucial technique for simplifying complex dynamics in chemical physics. While the AL (1) is equipped to address finding  $\Delta U$  as the slope of the semilog plot of  $\Phi_{\text{SP}}$ , building on the subexponential dependence on  $\tau_0$ , it is ill equipped to infer the number and positions of the metastabilities.

The problem of quantifying the state space of long-lived states was addressed in the literature, especially by employing statistical tools to assess the state space number, i.e. the number of local minima of the trapping potential or metastabilities. For instance, one key result in chemical kinetics, is that the randomness parameter or the coefficient of variation measured from the turnover time of an enzymatic reaction can place a strict lower limit on the topology i.e., the number of metastable kinetic states in any viable model for the mechanism of a given enzyme [19]. Another method based on escape time was proposed by Li and Kolomeisky [20] to determine the mechanism and topology of complex chemical and biological networks. There, the authors hypothesized that the short-time escape probability captures the number of metastabilities of the shortest path that the system's transition path takes. Recently, this theoretical work was tested in a high precision experiment [14], for an overarching set of complex molecular or nanoscale systems to unravel the quantitative features of the underlying energy landscape. In another work, the structure of the protein folding energy landscape involving multiple kinetic traps was predicted via the multiple relaxation time scales emanating from the first passage time distribution between reactants and products of these biomolecules [21]. In a

\* [arnabpal@imsc.res.in](mailto:arnabpal@imsc.res.in)

† [ohads@sci.haifa.ac.il](mailto:ohads@sci.haifa.ac.il)

similar vein, our key goal here is to uncover the details of the potential landscape from the perspective of the Arrhenius Law, generalized to interacting particle systems (2) thereby establishing a powerful and robust theoretical method irrespective of the complex underlying mechanisms.

Particles with excluded volume interactions, positioned in a deep trap, acquire the escape rate given by the many-body Arrhenius law [22, 23]

$$\Phi_{\text{MP}} \asymp \exp(-\beta\Delta U g), \quad (2)$$

where  $\Delta U g$  is an effective activation energy [24]. The term  $g$  depends on the particle density in the trap and is computable for an arbitrary trapping potential, using a geometrical argument. Notably  $g$  is found to be independent of the inter-particle interactions aside from the excluded volume. In this work, we show that varying  $g$  as a function of the particle density in the trap results in kinks associated with the local minima and maxima of the trap potential (see Fig. 1). We reveal a surprising equivalency between  $\Phi_{\text{MP}}$  and a thermodynamic partition function. Drawing on the theory of critical phenomena, we construct analogous thermodynamic response functions as quantitative tools to detect metastabilities, treating them as the counterparts of thermodynamic phase transitions.

## SETUP

To make matters more concrete, let us introduce a setup à la Kramers in one dimension. We confine an interacting gas consisting of  $M$  excluded volume particles in a trap of size  $L$ , with  $X$  denoting the position in the trap. We introduce the rescaled potential  $U(x)$ , where  $x = X/L \in [0, 1]$ . The trap potential has a global minimum at  $x = 0$ . We fix  $U(0) = 0$  for convenience, and impose a reflecting boundary condition at  $x = 0$ . At  $x = 1$ , the potential has a global maximum, fixing  $U(1) = \Delta U$ , and imposing an absorbing boundary condition. We are interested in the mean escape time, i.e. the mean time it takes for the fastest particle to reach the absorbing boundary at  $X = L$  for the first time. In this work, we focus on deep potential traps, i.e.  $\beta\Delta U \gg 1$ , where the mean escape time is long, and as large deviation theory becomes relevant, the mean escape time converges to  $1/\Phi_{\text{MP}}$ . In the limit of large  $M, L$ , with a fixed particle density in the trap  $\bar{\rho} = M/L$  [23, 25], we find (2). The form of  $g$  in (2) is explicitly given by  $g = 1 - U_{\text{top}}/\Delta U$ , with  $U_{\text{top}}$  defining the maximum potential value occupied by particles (see Fig. 2). This implies

$$\bar{\rho} = \int dx \Theta(U_{\text{top}} - U(x)), \quad (3)$$

where  $\Theta$  is the Heaviside function.

Eq. (2) is non-trivial to derive in the many-body case, yet, it can be understood by an intuitive argument. In the limit  $\beta\Delta U \rightarrow \infty$ , the particles organize into

the minimal (free) energy configuration (MEC), which is primarily determined by the structure of the potential (see Fig. 2). The escaping particle is the one with the highest potential energy,  $U_{\text{top}}$  in the MEC (also see [8]). This intuition essentially leads to (2), recalling that  $g = 1 - U_{\text{top}}/\Delta U$ . Note that activating a single particle from the MEC leads to an energy dominated free energy change in the macroscopic system. The latter assertion may differ for particles with long-range interactions like polymers [26] which we do not consider within our formalism.

The MEC was shown to correctly predict  $g$  for a set of important diffusive lattice gas models [22, 23], where the potential was taken to be monotonous. Within our trap setup, and for monotonous potentials, the MEC predicts via (3) that  $U_{\text{top}} = U(x = \bar{\rho})$ , leading to

$$g_{\text{monotone}}(\bar{\rho}) = 1 - U(x = \bar{\rho})/\Delta U. \quad (4)$$

See also Fig. 2. Intuitively, the escape rate should increase as we fill the trap with excluded volume particles, since adding particles pushes the highest energy particle in the trap closer to the activation energy. Hence,  $g$  has to be a monotonous decreasing function of  $\bar{\rho}$ . From this reasoning alone, it is clear that  $g$  cannot follow (4) for non-monotonous potentials. The presence of non-monotonous potentials is quite ubiquitous in the context of particle, ion or metabolite transport through confined geometries containing narrow openings, corners, bottle-necks or channels. Despite their pervasiveness, the inverse problem of inferring the structure of the channel, the nature of the potential from the escape time statistics remains a challenge [21]. In what follows we analyze the structure of  $g$  for an arbitrary non-monotonous potential, and show the relevance to the inference problem.

## EMERGENCE OF THE KINKS

In non-monotonous potentials, the escape rate, and in particular  $g(\bar{\rho})$  varies dramatically from the monotonic case captured in (4). Indeed, one still infers  $g$  from the MEC. Before providing  $g$  for an arbitrary trapping potential, it is instructive to first consider a minimal model for a non-monotonous potential – the piecewise linear potential (see Fig. 3). Recall that  $g = 1 - U_{\text{top}}/\Delta U$  for any arbitrary potential. However, crucially  $U_{\text{top}} \neq U(x = \bar{\rho})$  for the non-monotonous potentials. Now, one may proceed by determining  $U_{\text{top}}(\bar{\rho})$ , or alternatively the inverted function  $\bar{\rho}(U_{\text{top}})$  from (3), the latter leads to

$$\bar{\rho}(U_{\text{top}}) = \begin{cases} \frac{U_{\text{top}}}{2\Delta U}, & \text{for } 0 < \frac{U_{\text{top}}}{\Delta U} < \frac{1}{3} \\ 2\frac{U_{\text{top}}}{\Delta U} - \frac{1}{2}, & \text{for } \frac{1}{3} < \frac{U_{\text{top}}}{\Delta U} < \frac{2}{3} \\ \frac{U_{\text{top}}}{\Delta U} + \frac{1}{2}, & \text{for } \frac{2}{3} < \frac{U_{\text{top}}}{\Delta U} < 1. \end{cases} \quad (5)$$

It should then be understood that the kinks in  $\bar{\rho}(U_{\text{top}})$  correspond to the local minimum and maximum of  $U_{\text{pwl}}$ .

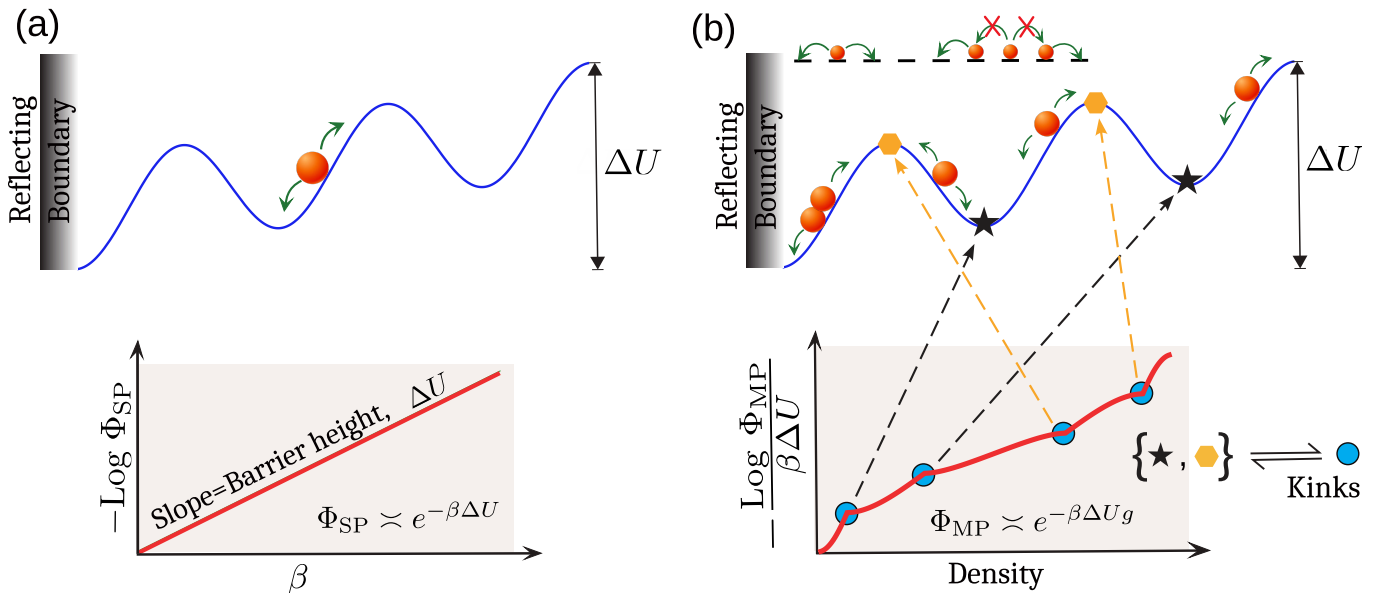


FIG. 1. (a) The escape problem of a single particle. The bottom figure shows the traditional inference of the activation barrier height from Arrhenius law (1) (b) Inference of the potential minima and maxima by employing the many-body Arrhenius law (2). The number of kinks in the bottom figure correspond to local maxima and minima of the potential  $U(x)$  in the middle figure. Thus, the many-body escape dynamics (for instance, activated dynamics of a stochastic lattice gas model with volume exclusion as shown in the top) allow to infer the metastabilities of the single particle escape problem.

These kinks would be inherited by  $g(\bar{\rho})$ . Recalling  $g(\bar{\rho}) = 1 - U_{\text{top}}/\Delta U$ , one can invert (5), to find (see Fig. 3)

$$1 - g(\bar{\rho}) = \begin{cases} 2\bar{\rho} & \text{for } 0 < \bar{\rho} < \frac{1}{6} \\ \frac{1}{2}\bar{\rho} + \frac{1}{4} & \text{for } \frac{1}{6} < \bar{\rho} < \frac{5}{6} \\ 2\bar{\rho} - 1 & \text{for } \frac{5}{6} < \bar{\rho} < 1 \end{cases} \quad (6)$$

The treatment above for  $U_{\text{pwl}}$  can be generalized to an arbitrary potential trap. It is the local minima and maxima of the potential trap that introduce kinks in  $g(\bar{\rho})$ . Let  $n$  be the number of intersections of  $U_{\text{top}}$  with an arbitrary trapping potential  $U(x)$ . Unless  $U_{\text{top}}$  exactly intersects with a local maximum or minimum point,  $n = 2m + 1$  is an odd number larger or equal to one. The MEC implies that

$$\bar{\rho}(U_{\text{top}}) = \sum_{i=0}^m (x_{2i+1} - x_{2i}), \quad (7)$$

where  $x_0 = 0$  and  $x_i$  is the  $i$ -th intersection of  $U(x)$  with  $U_{\text{top}}$  (Fig. 2 (b) demonstrates the idea). The function  $\bar{\rho}(U_{\text{top}})$  changes non-analytically as  $U_{\text{top}}$  crosses a local minima and maxima. This is the source of the kinks in  $g(\bar{\rho})$ , and the number of kinks corresponds to the number of local minima and maxima of the potential  $U$ . It should be noted that it is hard in general to provide an analytic expression of  $g(\bar{\rho})$  as it involves finding analytically the intersections of the arbitrary trap potential  $U(x) = U_{\text{top}}$  for any  $0 < U_{\text{top}} < 1$ , and then invert (7). Nevertheless, a numerical inference of  $g$  is straight-forward for any arbitrary trap potential and at any desired level of precision.

Thus, we are able to represent  $g$  for both monotonous and non-monotonous trap potentials using the MEC.

## THE KINKS AND THERMODYNAMIC PHASE TRANSITIONS

Importantly, the MEC and the resulting kinks are obtained as asymptotic results in the  $\beta\Delta U \rightarrow \infty$  limit. The kinks constitute dynamical phase transitions as the mean density is varied. However, the escape rate  $\Phi_{\text{MP}}$ , or  $g$ , are expected to be analytic at finite  $\beta\Delta U$ . To build this intuition, let us draw a correspondence between the kinks in the escape problem to the critical phenomena in thermodynamics. A thermodynamic phase transition points to a non-analyticity in the thermodynamic potential, say the Helmholtz Free energy, when the temperature is varied beyond a critical temperature. The non-analytic point is apparent only in the thermodynamic limit of an infinite system. Translating to the MEC, the *large system size* in thermodynamics corresponds to the  $\beta\Delta U \rightarrow \infty$  limit and the *temperature* corresponds to the mean density  $\bar{\rho}$ , which can be externally controlled. Bridging this correspondence, we can define

$$\mathcal{F} = -\frac{1}{\beta\Delta U} \log \Phi_{\text{MP}}, \quad \mathcal{R}_n = \frac{\partial^n \mathcal{F}}{\partial \bar{\rho}^n} \quad (8)$$

to correspond to the free energy per volume, where  $\beta\Delta U$  serves as the volume parameter and  $\mathcal{R}_n$  are the associated response functions.

Crucially, the non-analytic nature of the escape rate becomes apparent only in the *thermodynamic limit*, i.e.

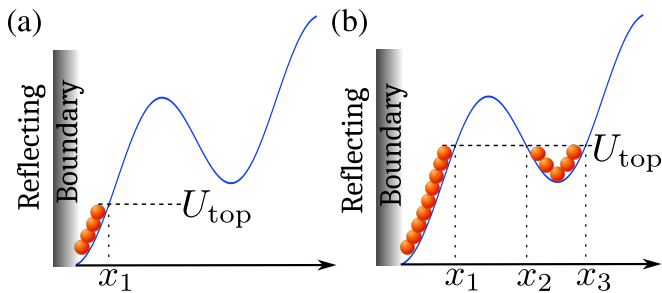


FIG. 2. A visualization of the MEC for particles with excluded volume on an arbitrary non-monotonic potential. Particles occupy the potential for  $U(x) < U_{\text{top}}$ . (a) Here  $U_{\text{top}}$  is smaller than the lowest value of the potential extrema. Thus,  $U_{\text{top}}$  has a single intersection with  $U(x)$ , at position  $x_1$ , and we find  $\bar{\rho}(U_{\text{top}} = U(x_1))$ , leading to  $U_{\text{top}}(\bar{\rho}) = U(x = \bar{\rho})$  as in the monotonous potential. (b) Here  $U_{\text{top}}$  is in the range where there are three intersection points with  $U(x)$ , denoted by  $x_{1,2,3}$ . In this case  $\bar{\rho}(U_{\text{top}}) = x_1 + x_3 - x_2$ . Notice that in this case  $U_{\text{top}}(\bar{\rho}) \neq U(x = \bar{\rho})$ .

at  $\beta\Delta U \rightarrow \infty$ . At finite  $\beta\Delta U$ , it is especially hard to observe the emerging kinks, as  $\beta\Delta U$  is rather limited experimentally to order of 50, contrary to the macroscopic volume in thermodynamic systems [27]. A standard method to observe phase transition is by measuring the scaling of response functions such as susceptibilities and other derivatives of the thermodynamic potentials. This essentially corresponds to looking at the derivatives of  $\mathcal{F}$  and the scaling of the divergences close to the critical densities, i.e. where we expect the kinks. That is, instead of the MEC, it is required to determine  $\Phi_{\text{MP}}$  for a finite  $\beta\Delta U$ . This has been achieved in [23], by developing a perturbative approach, estimating  $g$  analytically at a finite (but large)  $\beta\Delta U$  [28].

### RESPONSE FUNCTIONS FOR AN INTERACTING LATTICE GAS MODEL

To demonstrate the emergence of the kinks through the response functions, we focus on the simple exclusion process (SEP) [29, 30]. The SEP is a paradigm in the study of nonequilibrium physics, capturing the behavior of stochastic transport of biomolecules and molecular motors through complex media, surface growth, vehicular traffic and more [29, 31, 32].

The SEP describes a jump process, where particles jump to neighboring empty lattice sites only thus ensuring an excluded volume interaction. To find the finite size  $\beta\Delta U$  escape rate, Ref [23] uses a hydrodynamic theory – the macroscopic fluctuation theory [33–35] – to handle the inter-particle interactions. The theory shows that one needs to find the typical density profile that maximizes the probability that all the particles survive in the trap. To that end, it was proposed in [23] to consider a perturbative approach. First, consider the equilibrium density profile in the box with reflecting boundary

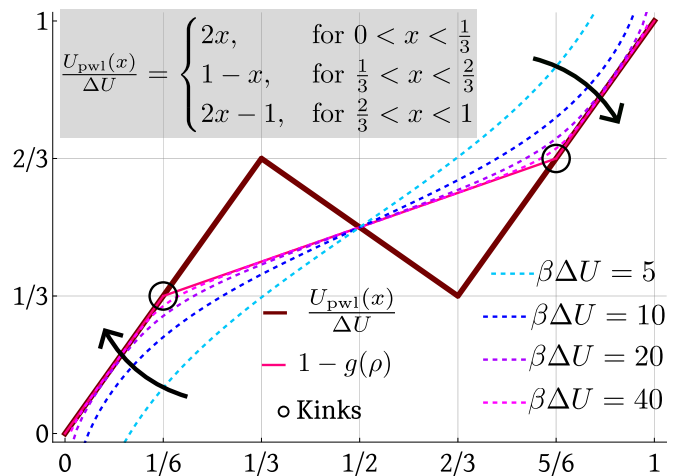


FIG. 3. (Top) The piecewise linear potential  $U_{\text{pwl}}(x)$  is plotted (solid thick brown) together with the MEC prediction for  $1-g$  (solid magenta). The black circles highlight the positions of the kinks in  $g$ . The dashed lines reveal the convergence of the finite  $\beta\Delta U$  approximation scheme to the MEC  $1-g$  curve. Noticeably, the convergence, marked by the black arrows, is faster away from the kinks.

conditions. In this case, the density at the right hand side does not vanish as it should for an absorbing boundary condition. However, the equilibrium density at the boundary is small due to the high value of the potential  $\beta U(x=1) = \beta\Delta U$ . So, the typical density profile can be obtained by adding a small perturbation to the equilibrium density profile, which takes care of the absorbing boundary discrepancy.

We start with the general expression for the escape rate namely  $\Phi_{\text{MP}} \asymp e^{-\beta\Delta U} A$ , as derived in [23]. Here, one can infer  $A$  from the value of the equilibrium density profile at the absorbing boundary using the following relation [27]

$$1 - \bar{\rho} = \int dx \frac{1}{1 + Ae^{-\beta U(x)}}, \quad (9)$$

for a given  $U(x)$ . For the SEP particles in a piecewise linear potential  $U_{\text{pwl}}$ , Eq. (9) can be solved to get an expression for  $A$  in the “finite size” limit, revealing the precursor to the criticality in the escape rate in the “finite size” limit [27]. For brevity, we will examine the regime  $0 < \bar{\rho} < 1/6$  where the finite size expression of  $A$  (and thus the escape rate) can be made simpler [27]. However, the analysis could be extended to the full range of  $\bar{\rho}$ , doing so in the main text would introduce technical complexity, going against our pedagogical purposes. Thus, we provide a full numerical analysis of the piecewise linear potential in [27].

We can now write the corresponding free-energy in the finite size limit following (8)

$$\begin{aligned} \mathcal{F} &= \mathcal{F}_0 + \mathcal{F}_s, \\ \mathcal{F}_s &= -\frac{1}{\beta\Delta U} \log \frac{-1 + \sqrt{1 + 12e^{-\epsilon\beta\Delta U}}}{6}, \end{aligned} \quad (10)$$

where  $\epsilon/2 = 1/6 - \bar{\rho}$  measuring the distance from the critical density  $\bar{\rho} = 1/6$ . Here  $\mathcal{F}_0 = 2/3$  is a regular contribution that will not lead to the divergence of the response functions. We note that there are subleading terms in  $\mathcal{F}_0$ , that are discarded in our perturbative approach.  $\mathcal{F}_s$  is the singular part of the associated free energy. The singularity appears at  $\epsilon\beta\Delta U \rightarrow \infty$  which corresponds to a finite  $\epsilon$  (distance from the critical density) and infinite  $\beta\Delta U$ . It is then clear that observing the singularity directly from  $\mathcal{F}$  is impractical. In other words, the formation of the kinks will become apparent only at exceptionally large values of  $\beta\Delta U \approx 100$ . Therefore, to observe the precursors of the kinks, we turn to the response functions. The response functions accentuate the singular part of  $\mathcal{F}$ , i.e.  $\mathcal{R}_n \propto (\beta\Delta U)^{n-1}$  when keeping  $z$  finite. Fig. 4 demonstrates our findings. We first show that while  $\mathcal{F}$  converges to its MEC value as we increase  $\beta\Delta U$ , the convergence is slower close to the critical point, i.e. for  $\epsilon \rightarrow 0$ . Moreover, we demonstrate the scaling behavior of the response function  $\mathcal{R}_2$ .

Finding an analytical expression for  $\mathcal{F}$  for arbitrary potential landscape turns out to be completely intractable, even for the SEP within the perturbative approach. Nevertheless, inference of the kinks through the response functions is not limited to an analytic treatment alone, but can be probed using numerical techniques using the response functions. This is demonstrated in [27] for non-linear trap potentials with multiple metastabilities – the appearance of similar potential energy barriers in the activation gating of the bacterial ion channels is quite ubiquitous [36]. It is demonstrated in [27] how  $\mathcal{F}$  systematically converges to the MEC limit in the large  $\beta\Delta U$  limit while the response functions clearly indicate the emergence of the kinks. In a nutshell, the local minima and maxima of the potential can be inferred from the response functions, obtained from escape time measurements, without prior knowledge of the trap potential.

## DISCUSSION

In this work, we have revisited the survival probability of interacting particles located in a deep trap potential. The particle escape rate follows the generalized Arrhenius form  $\Phi_{\text{MP}} \asymp e^{-\beta\Delta U g}$ , where  $g$  can be asymptotically assessed via the MEC. It was shown that in the excluded volume universality, i.e. for lattice gas models where the lattice site occupancy is capped,  $g(\bar{\rho})$  becomes singular in  $\beta\Delta U \rightarrow \infty$  when the trap potential introduces local minima and maxima. More precisely, local maxima and minima of the trap potential lead to kinks in  $g(\bar{\rho})$ . Thus, reversing the logic, measurement of kinks in the many-body  $g$  allows to infer the number and positions of the single particle long-lived states (metastabilities) induced by the trap potential local minima. The salient point of this work is proposing a statistical test, based on the measurable mean escape time of the many-body problem, that allows to quantify the number of long-lived

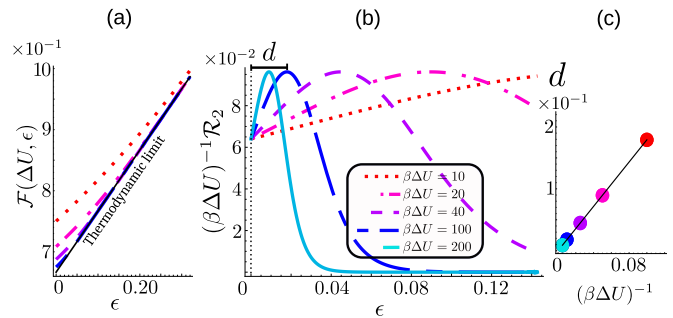


FIG. 4. (a) The “free energy”  $\mathcal{F}$  is calculated for finite  $\beta\Delta U$  values, and compared with the MEC result ( $\beta\Delta U = \infty$ ) for SEP particles subjected to the  $U_{\text{pwl}}$  trapping potential. It is evident that convergence is better away from the critical point at  $\epsilon = 0$ . However, to infer the criticality, we need to consider the response function  $\mathcal{R}_2$ . (b) The rescaled response function  $\mathcal{R}_2/(\beta\Delta U)$  for different  $\beta\Delta U$  as found from Eq. (10). The precursor of the kink manifest as a scalable peak, at distance  $1/\beta\Delta U$  from the expected kink. (c) The distance  $d$  of the peaks from the expected critical point is shown to scale like  $1/\beta\Delta U$ .

states in the single-particle activation problem.

Statistical physics states that finite systems can only lead to analytic thermodynamic observables. Therefore, phase transitions occur only in the thermodynamic limit of infinite system size. However, for a macroscopic particle number of the order of Avogadro’s number, it is hard to tell the difference between a true divergence of, e.g. the response functions, and a large but finite increase close to the critical point. Here,  $\beta\Delta U$  serves as the equivalent of the system size, whereas the density serves as the control parameter to manipulate towards the critical points. This implies that observing the kinks experimentally is unattainable. It is more practical to focus on the scaling properties of the diverging response functions. To see that, we recall that

$$\begin{aligned} \mathcal{F} &= -g(\bar{\rho}) + \mathcal{F}_s \\ &+ \text{non-singular subleading terms,} \\ \mathcal{F}_s &= \Delta U^{-\alpha} f_s(\Delta U \delta \rho^\gamma). \end{aligned} \quad (11)$$

The regular part is dominated by  $g$  at large  $\beta\Delta U$ , and the singular part is given by a singular scaling function  $f_s$ . Here  $\delta\rho$  is the distance from the critical density, and  $\alpha, \gamma > 0$  are critical exponents. In the two examples considered here, we found  $\alpha = \gamma = 1$ . We could not show that this should always be the case. However, the inference of the kinks hardly depends on the exact value of the critical exponents [27].

As a proof of concept, it was demonstrated that this approach allows to infer the position of the kinks in both an analytically solvable model (the piecewise linear potential) and through numerical investigation in the two extrema potential. In [27], we analyze a potential with four local extrema, and show that our method works there as well. It is important to stress that there are

obvious limits to the method. For example, if two extremal points in the potential are in close proximity, or if the trap potential introduces a very rugged landscape, the sharpness of the response function scaling test is reduced.

Experimentally, we expect our method to be useful in analyzing transport of interacting particles through a narrow channel, and against a potential gradient. The robust experimental setup by [14] et al. that recently designed colloid transport in the presence of multiple traps by an optical tweezers setup could be a potential avenue to validate our method. Within this setup, collecting measurements on the particle escape rates at different particle densities would allow us to predict the number of local extrema of the potential gradient.

In this work, we have restricted the trap potential to  $1D$ . Nevertheless, we point out that the treatment can be extended to higher dimensions, as well as to multi-

channel activation problems. It would be interesting to consider also non-diffusive activation processes introducing interacting systems [37, 38], as well as particles with soft interactions, going beyond lattice gas models [39, 40]. Finally, it may be interesting to apply novel approaches to use the finite  $\beta\Delta U$  scaling close to the critical points of the escape rate  $\Phi_{MP}$  in order to obtain better predictions of the behavior away from the criticality [41].

**Acknowledgments.**— The numerical calculations reported in this work were carried out on the Nandadevi and Kamet cluster, which are maintained and supported by the Institute of Mathematical Science’s High-Performance Computing Center. AP gratefully acknowledges research support from the Department of Atomic Energy, Government of India via Soft Matter Apex projects. OS gratefully acknowledges useful discussions on the experimental aspects of the work with Yael Roichman and Felix Ritort.

- 
- [1] P. Hänggi, P. Talkner, and M. Borkovec, Reaction-rate theory: fifty years after kramers, *Reviews of Modern Physics* **62**, 251 (1990).
- [2] E. Woillez, Y. Zhao, Y. Kafri, V. Lecomte, and J. Tailleur, Activated escape of a self-propelled particle from a metastable state, *Physical Review Letters* **122**, 258001 (2019).
- [3] E. Woillez, Y. Kafri, and N. S. Gov, Active trap model, *Physical Review Letters* **124**, 118002 (2020).
- [4] D. Mukamel, S. Ruffo, and N. Schreiber, Breaking of ergodicity and long relaxation times in systems with long-range interactions, *Physical Review Letters* **95**, 240604 (2005).
- [5] E. Saadat, I. Latella, and S. Ruffo, Lifetime of locally stable states near a phase transition in the thirring model, *arXiv preprint arXiv:2305.03009* (2023).
- [6] P. Krapivsky, K. Mallick, and T. Sadhu, Large deviations in single-file diffusion, *Physical Review Letters* **113**, 078101 (2014).
- [7] L. Berthier and G. Biroli, Theoretical perspective on the glass transition and amorphous materials, *Reviews of modern physics* **83**, 587 (2011).
- [8] J. S. Langer, Statistical theory of the decay of metastable states, *Annals of Physics* **54**, 258 (1969).
- [9] A. Dubkov, C. Guarcello, and B. Spagnolo, Enhancement of stability of metastable states in the presence of  $1/e$  vy noise, *arXiv preprint arXiv:2311.13464* (2023).
- [10] I. del Amo and P. Ditlevsen, Escape by jumps and diffusion by  $\{\alpha\}$ -stable noise across the barrier in a double well potential, *arXiv preprint arXiv:2308.05684* (2023).
- [11] K. Neupane, D. A. Foster, D. R. Dee, H. Yu, F. Wang, and M. T. Woodside, Direct observation of transition paths during the folding of proteins and nucleic acids, *Biophysical Journal* **110**, 517a (2016).
- [12] M. Chupeau, J. Gladrow, A. Chepelianskii, U. F. Keyser, and E. Trizac, Optimizing brownian escape rates by potential shaping, *Proceedings of the National Academy of Sciences* **117**, 1383 (2020).
- [13] H. Yu, X. Liu, K. Neupane, A. N. Gupta, A. M. Brigley, A. Solanki, I. Sosova, and M. T. Woodside, Direct observation of multiple misfolding pathways in a single prion protein molecule, *Proceedings of the National Academy of Sciences* **109**, 5283 (2012).
- [14] A. L. Thorneywork, J. Gladrow, Y. Qing, M. Rico-Pasto, F. Ritort, H. Bayley, A. B. Kolomeisky, and U. F. Keyser, Direct detection of molecular intermediates from first-passage times, *Science Advances* **6**, eaaz4642 (2020).
- [15] A. L. Thorneywork, J. Gladrow, U. F. Keyser, M. E. Cates, R. Adhikari, and J. Kappler, Resolution dependence of most probable pathways with state-dependent diffusivity, *arXiv preprint arXiv:2402.01559* (2024).
- [16] B. R. Ferrer and J. R. Gomez Solano, Experimental measurement of mean transition path velocities of colloidal particles surmounting energy barriers, *New Journal of Physics*.
- [17] F. Ginot, J. Caspers, M. Krüger, and C. Bechinger, Barrier crossing in a viscoelastic bath, *Physical Review Letters* **128**, 028001 (2022).
- [18] D. E. Makarov, *Single molecule science: physical principles and models* (CRC Press, 2015).
- [19] J. R. Moffitt, Y. R. Chemla, and C. Bustamante, Methods in statistical kinetics, in *Methods in enzymology*, Vol. 475 (Elsevier, 2010) pp. 221–257.
- [20] X. Li and A. B. Kolomeisky, Mechanisms and topology determination of complex chemical and biological network systems from first-passage theoretical approach, *The Journal of chemical physics* **139** (2013).
- [21] D. J. Wales, Dynamical signatures of multifunnel energy landscapes, *The Journal of Physical Chemistry Letters* **13**, 6349 (2022).
- [22] V. Kumar, A. Pal, and O. Shpielberg, Arrhenius law for interacting diffusive systems, *Physical Review E* **109**, L032101 (2024).
- [23] V. Kumar, A. Pal, and O. Shpielberg, Emerging universality classes in thermally assisted activation of interacting diffusive systems: A perturbative hydrodynamic approach, *The Journal of Chemical Physics* **160** (2024).
- [24] Here  $\asymp$  suggests asymptotic equivalence, discarding sub-exponential corrections.

- [25] D. Hartich and A. Godec, Duality between relaxation and first passage in reversible markov dynamics: rugged energy landscapes disentangled, *New Journal of Physics* **20**, 112002 (2018).
- [26] K. Sebastian and A. K. Paul, Kramers problem for a polymer in a double well, *Physical Review E* **62**, 927 (2000).
- [27] See Supplemental Material for detailed derivations, simulation details and other additional explanations.
- [28] In [22], an exact approach was developed. However, the treatment is much harder analytically, and numerically the estimation is limited to about  $\beta\Delta U = 20$ .
- [29] K. Mallick, The exclusion process: A paradigm for non-equilibrium behaviour, *Physica A: Statistical Mechanics and its Applications* **418**, 17 (2015).
- [30] B. Derrida, Non-equilibrium steady states: fluctuations and large deviations of the density and of the current, *Journal of Statistical Mechanics: Theory and Experiment* **2007**, P07023 (2007).
- [31] T. Chou, K. Mallick, and R. K. Zia, Non-equilibrium statistical mechanics: from a paradigmatic model to biological transport, *Reports on progress in physics* **74**, 116601 (2011).
- [32] C. Appert-Rolland, J. Cividini, and H. Hilhorst, Frozen shuffle update for an asymmetric exclusion process on a ring, *Journal of Statistical Mechanics: Theory and Experiment* **2011**, P07009 (2011).
- [33] L. Bertini, A. De Sole, D. Gabrielli, G. Jona-Lasinio, and C. Landim, Macroscopic fluctuation theory, *Reviews of Modern Physics* **87**, 593 (2015).
- [34] T. Agranov and B. Meerson, Narrow escape of interacting diffusing particles, *Physical Review Letters* **120**, 120601 (2018).
- [35] O. Shpielberg, T. Nemoto, and J. Caetano, Universality in dynamical phase transitions of diffusive systems, *Physical Review E* **98**, 052116 (2018).
- [36] T. Linder, B. L. de Groot, and A. Strydom, Probing the energy landscape of activation gating of the bacterial potassium channel kcsa, *PLOS Computational Biology* **9**, e1003058 (2013).
- [37] B. Doyon, G. Peretto, T. Sasamoto, and T. Yoshimura, Ballistic macroscopic fluctuation theory, *SciPost Physics* **15**, 136 (2023).
- [38] C. Bernardin and R. Chetrite, Macroscopic fluctuation theory for ginzburg-landau dynamics with long range interactions, *arXiv preprint arXiv:2405.08212* (2024).
- [39] R. Dandekar, P. Krapivsky, and K. Mallick, Dynamical fluctuations in the riesz gas, *Physical Review E* **107**, 044129 (2023).
- [40] S. Santra, J. Kethepalli, S. Agarwal, A. Dhar, M. Kulkarni, and A. Kundu, Gap statistics for confined particles with power-law interactions, *Physical Review Letters* **128**, 170603 (2022).
- [41] D. Hathcock and J. P. Sethna, Phase transitions beyond criticality: extending ising universal scaling functions to describe entire phases, *arXiv preprint arXiv:2402.18531* (2024).